Physical Communication 17 (2015) 94–106

Contents lists available at ScienceDirect

Physical Communication

journal homepage: www.elsevier.com/locate/phycom

Full length article

Error exponent analysis of energy-based Bayesian decentralized spectrum sensing under fading☆

Sanjeev Gurugopinath *, Chandra R. Murthy, Vinod Sharma

Department of ECE, Indian Institute of Science, Bangalore, 560 012, India

ARTICLE INFO

Article history:
Received 18 July 2014
Received in revised form 16 July 2015
Accepted 21 August 2015
Available online 7 September 2015

Keywords:
Cognitive radio
Energy detection
Error exponents
Spectrum sensing

ABSTRACT

This paper considers decentralized spectrum sensing, i.e., detection of occupancy of the primary users' spectrum by a set of Cognitive Radio (CR) nodes, under a Bayesian set-up. The nodes use energy detection to make their individual decisions, which are combined at a Fusion Center (FC) using the K-out-of-N fusion rule. The channel from the primary transmitter to the CR nodes is assumed to undergo fading, while that from the nodes to the FC is assumed to be error-free. In this scenario, a novel concept termed as the *Error Exponent with a Confidence Level* (EECL) is introduced to evaluate and compare the performance of different detection schemes. Expressions for the EECL under general fading conditions are derived. As a special case, it is shown that the conventional error exponent both at individual sensors, and at the FC is zero. Further, closed-form lower bounds on the EECL are derived under Rayleigh fading and lognormal shadowing. As an example application, it answers the question of whether to use pilot-signal based narrowband sensing, where the signal undergoes Rayleigh fading, or to sense over the entire bandwidth of a wideband signal, where the signal undergoes lognormal shadowing. Theoretical results are validated using Monte Carlo simulations.

1. Introduction

Spectrum sensing, or the detection of the presence or absence of a primary signal in a given frequency band of interest, is a well-studied topic in literature on Cognitive Radios (CR) [1]. Multi-sensor detection, or decentralized detection, is the preferred approach for spectrum sensing, because of its resilience to signal fading, the hidden node problem, etc. [2–7]. In fixed sample-size decentralized detection, individual CR nodes make one-bit decisions about the availability of the spectrum using a given number of samples, and the individual decisions are combined at a Fusion Center (FC) to detect the presence or absence of the primary signal, possibly over a lossy channel [8]. Alternatively, the individual nodes can send multi-bit information about the decision statistic, which could be combined using soft-combining schemes such as the equal gain and maximal ratio combining [9–11], over a dedicated control channel or through physical layer fusion. Energy-based detection, popularly referred to as Energy Detection (ED), is a well known technique for spectrum sensing, wherein the signal energy in the band of interest is measured and compared with a threshold [12–16]. The primary signal is declared to be present if the measured energy exceeds the threshold.

The detection probability performance of ED when the channel between the primary transmitter and the secondary node undergoes narrowband Rayleigh fading has been analyzed under the Neyman–Pearson (NP) framework [13,14,17]. Although closed-form expressions for the probability of detection have been derived, due to the form

☆ This work has appeared in part in [50].

* Corresponding author.
E-mail addresses: sanjeev.g@ece.iisc.ernet.in (S. Gurugopinath), cmurthy@ece.iisc.ernet.in (C.R. Murthy), vinod@ece.iisc.ernet.in (V. Sharma).

http://dx.doi.org/10.1016/j.phycom.2015.08.005
1874-4907/

of the integrals involved, it is cumbersome to obtain the detection threshold that meets a given minimum detection probability requirement. One way around this is to use an alternative performance metric such as the error exponent [18,19], which essentially captures the asymptotic behavior of the probability of error performance of a detector as the number of samples used for making decisions gets large.[1] Mathematically, the error exponent is defined as $\lim_{M\to\infty} -\log(P_e)/M$, where M is the number of samples used for detection, and P_e is the corresponding probability of error. One of the early studies on the error exponent performance of decentralized detection was the seminal work of Tsitsiklis [20]. In the Bayesian framework, the exponent on the probability of error of decentralized detection has been analyzed in [21]. The Bayesian error exponent of mismatched likelihood ratio detectors was derived in [22]. The analysis uses the fact that the best achievable exponent in the Bayesian probability of error is the Chernoff information between the probability distribution functions under the two hypotheses. In turn, this implies that the optimal exponents associated with the probability of false alarm and the probability of missed detection must equal each other [19, Chap. 11], [23,24]. When the primary signal power or the noise variance at the secondary receiver are unknown, a robust and blind detection scheme based on the maximum eigenvalue of the sample covariance matrix has been proposed and studied through simulations [25]. In [26,27], multi-antenna assisted spectrum sensing is considered under the NP framework.

Decentralized detection for spectrum sensing under the Bayesian framework is considered in [28–30]. Here, the channel between the primary transmitter and the secondary sensors is assumed to undergo fading, while the channel between the sensors and the FC is assumed to be lossless but finite-rate. However, to the best of our knowledge, prior to this study, error exponents for energy-based decentralized spectrum sensing have not been derived in the literature. There are several advantages in using the error exponent as a performance metric under a Bayesian set-up. First, the optimal error exponent is independent of the specific values of the prior probabilities, provided they are nonzero [19]. Due to this, the optimal error exponent, and detection schemes based on maximizing the error exponent, are naturally robust to uncertainties in the knowledge of the prior probabilities, unlike detectors designed with the goal of minimizing the probability of error. Further, error exponents allow one to contrast the performance of competing detectors over a range of target performance requirements, rather than at a single missed detection probability target.[2] This is useful when choosing between detectors at the design phase of a hardware implementation.

[1] The number of samples can be considered to be large, for example, in Digital Television (DTV) signal detection, where the primary network changes its occupancy infrequently.

[2] For example, future primary networks may use receivers with better noise figures. In this case, to keep the interference caused to the primary network within acceptable limits, the CR receivers might need to sense for a longer duration in order to satisfy a (tighter) constraint on the detection error rate.

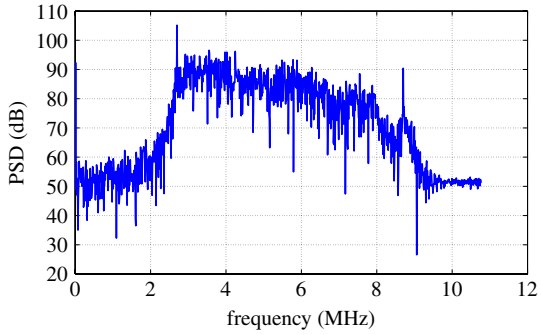

Fig. 1. One sided PSD of IEEE 802.22 DTV wideband signal.

Yet another reason for considering an error exponent analysis of spectrum sensing is related to the statistical properties of the fading experienced by the primary signal. For Narrow-Band (NB) signals, the multipath (Rayleigh) fading effect is dominant, in a non line-of-sight environment. On the other hand, Wide-Band (WB) signals span multiple coherence bandwidths, due to which, the Rayleigh fading component averages out when the signal energy is accumulated across the wideband, resulting in the lognormal shadowing as the dominant fading component [31–33]. As a concrete example, in the IEEE 802.22 (WRAN) standard, the primary (Digital Television (DTV)) signal is a wideband signal, with a strong pilot tone at 2.69 MHz (see Fig. 1).[3] There are therefore two options for detection. First, one could use an NB filter to capture just the pilot tone, and detect based on the pilot energy. This has the advantage of filtering out the WB noise; but the detector has to contend with a Rayleigh-faded NB signal. Alternatively, one could use the energy in the entire WB signal for detection, which averages out the Rayleigh fading [31,32], but the detector has to work against the lognormal shadowing and the added impairment due to the AWGN over the WB. Again, due to the complex form of the integrals involved, direct comparison of the two options using conventional performance metrics such as the probability of error is difficult. Hence, in this paper, we contrast these two options by analyzing the Bayesian error exponent performance of energy-based detection.

The main contributions of this work are as follows:

- The concept of *Error Exponent with a Confidence Level* (EECL) is introduced, which captures the largest exponent on the probability of error that can be achieved if a fraction $1-q$ (with $0 < q \leq 1$) of the worst channel states are discounted. The EECL at an individual sensor is derived for a large class of fading distributions. The traditional error exponent, which is a special case of the EECL as q approaches 1, is shown to approach 0 under general fading conditions.
- The EECL for decentralized detection with N sensors and when the FC uses the OR (1 out of N) rule is derived

[3] Note that, at the time of writing this paper, in the US, spectrum sensing is made optional in the IEEE 802.22 standard. However, in many countries other than the US and European countries, reliable databases may not be available [34]. In these cases, spectrum sensing is essential.

under the Rayleigh fading and lognormal shadowing channels. Also, the optimality of the OR rule among the class of K out of N fusion rules is established, in terms of the EECL.
- Closed-form lower bounds on the EECL are also derived, for both Rayleigh fading and lognormal shadowing channels. The bounds are easy to compute and become increasingly accurate as q approaches 1.
- The theoretical development is used to successfully address the question of NB versus. WB sensing, and a rigorous analysis is presented. Specifically, if the ratio of normalized NB and WB powers exceeds a threshold, then NB sensing is better than WB sensing in terms of the EECL, and vice versa.

We illustrate the efficacy of the EECL based design of spectrum sensing through Monte Carlo simulations. The EECL based design outperforms existing designs, in terms of the probability of error, when a small fraction of the worst channel states is discounted. Hence, the EECL based approach faithfully captures the performance of detectors in terms of the more commonly used performance metrics also. Further, due to its ease of computation, the EECL helps streamline the performance comparison between different detection strategies. The improved sensing performance can lead to better CR throughput and/or better primary user protection in CR implementations. Note that, joint design of the sensing scheme and the medium access protocol to maximize the secondary throughput [35,36], while an important topic of study, requires one to assume a specific model for the temporal behavior of the primary occupancy. Such a study is beyond the scope of this paper.

The rest of this paper is organized as follows. The problem set-up and the basics of error exponents are presented in Section 2. The EECL at a single node is introduced and analyzed in Section 3. Distributed detection is considered in Section 4, where the EECL at the FC with the OR rule is derived. The comparison between WB and NB spectrum sensing in terms of the EECL is discussed in Section 5. Simulation results are presented in Section 6, and Section 7 concludes the paper. Proofs of the theorems and corollaries are presented in the Appendix.

2. System model

We consider a decentralized detection set-up where N sensors use the average energy measured from M independent observations each as the test statistic for making their individual decisions between the signal absent (denoted $\mathcal{H}_0$) and signal present (denoted $\mathcal{H}_1$) hypotheses [37,26,2,38,39,3,4]. Such an energy-based test is known to be optimal when no knowledge about the structure of the primary signal is available at the CR nodes [12]. When M is large, using the Central Limit Theorem (CLT), the test statistic can be well-approximated as being Gaussian distributed, resulting in the following hypothesis test at each sensor [40,41][4]:

$$\mathcal{H}_0 : V_y \sim \mathcal{N}\left(0, \frac{1}{M}\right)$$

$$\mathcal{H}_1 : V_y \sim \mathcal{N}\left(|h|^2 P, \frac{1}{M}\right), \tag{1}$$

where $V_y \triangleq \frac{1}{M}\sum_{k=1}^{M} |Y_k|^2 - 1$ is the test statistic, and Y_k is the kth observation at the sensor. Also, $\mathcal{N}(\mu, \sigma^2)$ represents a Gaussian distribution with mean μ and variance σ^2. In writing the above, without loss of generality, we normalize the receiver noise variance to unity. The *average* received power of the primary signal, P, is assumed to be known at the nodes. The noise variance and average received signal power can be estimated, for example, using a calibration phase, when the primary signal is known to be absent and present, respectively.[5] Furthermore, for simplicity of presentation, we assume that the CR nodes are sufficiently close to each other that P is the same at all nodes [29,44]. In Section 4.1, we extend of the main results to the case where the average received powers at the CR nodes could be different. The channel gain, h, is assumed to be random, unknown, and constant for the M observations. Its distribution will be discussed later, and this distribution will be used in designing the test to minimize the probability of error, averaged over the channel statistics. In (1), we have omitted the sensor index from V_y for notational convenience, since the observations are assumed to be independent and identically distributed (i.i.d.) conditioned on the true hypothesis.

In the literature, various statistical models have been proposed for the channel h, depending on the signal bandwidth and propagation environment. As mentioned earlier, when the primary signal is NB, the Rayleigh fading component typically dominates the lognormal shadowing components, and hence $|h|^2$ can be modeled as exponentially distributed [45,46]. When the primary signal is a WB signal, it spans multiple coherence bandwidths, due to which, the Rayleigh fading components average out, resulting in h being a lognormal shadowing random variable [32,31]. Other models include the Nakagami-m distribution, the Weibull distribution, and the Suzuki distribution [31]. In this work, we focus on the two most commonly used models, namely, the Rayleigh and the lognormal shadowing distributions, for the NB and WB fading cases, respectively. We assume that the fading is i.i.d. across the sensor nodes. The case where the fading instantiation is spatially correlated (see, for e.g., [3,47]), is an interesting but independent problem, and is beyond the scope of this paper. However, we note that, under the i.i.d. fading assumption, our main results can be extended to handle any of the fading models mentioned above.

We assume that the sensors transmit their binary decisions to an FC through a finite rate, noiseless, delay-free CR control channel, as in [28,29]. This simplifies the analysis, and the corresponding EECL represents an upper bound on the error exponent achievable in the general case. It is

[4] The hypothesis test here is a slightly modified version of the tests in [40,41], in the sense that while the aforementioned references first construct the energy in the received samples as the test statistic and then apply the CLT to approximate its distribution, here we directly present the CLT-approximated statistics of the normalized received energy.

[5] In a more practical scenario, with an uncertainty in the estimate of the noise variance [40–43], the above test in (1) can be designed under a minimax criterion [23], and the detection threshold can be set such that the worst-case probability of error across the range of possible noise variance values is minimized. This corresponds to designing the threshold by considering the noise variance to be highest value within the uncertainty range.

valid when the CRs use a low-rate dedicated control channel to forward their decisions to the FC. The FC combines the individual decisions using the K out of N fusion rule to detect the presence or absence of the primary signal. It is known that, when the individual sensor decisions are i.i.d. conditioned on the true hypothesis, the K out of N fusion rule is optimal in terms of probability of error [23,48]. In particular, we will focus on the 1 out of N fusion rule, i.e., the OR fusion rule, in the sequel. We will show that the OR fusion rule has a certain optimality property in terms of the error exponents. In the next section, we present the main results on the EECL at an individual sensor. We extend it to multiple-node decentralized detection in Section 4.

3. Detection at the sensors

We start by considering the single-sensor hypothesis testing problem in (1). The conventional error exponent is defined as $\lim_{M\to\infty} \frac{-\log p_e}{M}$, where p_e denotes the probability of error at the sensor, and is given by $\pi_0 p_f + (1-\pi_0)p_m$, with π_0, p_f and p_m denoting the prior probability of hypothesis $\mathcal{H}_0$, the false alarm probability, and the missed detection probability, respectively. As mentioned earlier, in many practical applications, it is of interest to analyze the performance of detectors when the received signal power from the primary transmitter exceeds a threshold (for example, in the IEEE 802.22 standard, it is -116 dBm [49]). In terms of error exponents, this corresponds to studying the error exponent when a small fraction, say 0.1%, of the channel fade instantiations are ignored. Motivated by this, in this paper, we consider the EECL as a novel performance metric to evaluate and compare the performance of NB and WB spectrum sensing approaches [50]. Note that, the traditional error exponent is obtained as a special case of the EECL, as a parameter q defined in the sequel approaches unity. The EECL at a single sensor is mathematically defined below. We extend the definition to the N sensor case in the next section.

Definition 1. Let S_q denote a set of channel instantiations such that $\mathcal{P}\left(|h|^2 \in S_q\right) = q$. The *error exponent with a confidence level q*, denoted EECL(q), is the maximum error exponent achievable conditioned on $|h|^2 \in S_q$, where the maximization is over all possible choices of S_q.

Now, in the single sensor case, it is immediate to see that, among all possible choices for S_q, the highest error exponent is achieved by letting $S_q = \left\{|h|^2 : |h|^2 \geq |h_0|^2\right\}$, where the threshold $|h_0|^2$ depends on the minimum power level at which the primary signal detection performance needs to be guaranteed by the CR.

The EECL can also be used to compare NB vs. WB sensing when the detectors are designed, for example, to satisfy a given missed detection probability constraint, β, as follows. Pick $0 < \alpha < \beta$. For a fraction α of the channel states, the missed detection probability can be upper bounded by unity. For the remaining fraction $1-\alpha$ of the channel states, we set the detection threshold such that the missed detection probability is at most $\beta - \alpha$. Then, the overall missed detection probability is upper bounded by β. As will be shown in the sequel, discounting a fraction α of the channel states allows one to achieve a positive exponent on the probability of error. Hence, if one detection scheme has a larger EECL than another, the detector with the larger EECL will have a significantly smaller false alarm rate, and, consequently, better secondary throughput, for the given missed detection probability constraint of β, as the number of observations gets large. Hence, the EECL can be used as a metric for the design, and performance comparison, of different detection schemes.

The main result of this section is stated as the theorem below. It is valid as long as the distribution of the gain of the channel from the primary transmitter to the sensors is continuous and nonzero for infinitesimally small arguments. To obtain the result, we use the fact that, under a Bayesian setup, the optimal exponent on the probability of error is achieved when the exponents on the probabilities of false alarm and the missed detection are equal [19, Chap. 11], [23].

Theorem 1. *Let $\alpha \triangleq |h|^2$. The Bayesian hypothesis test defined in (1) achieves an EECL(q) of $\frac{(\alpha_0 P)^2}{8}$, where α_0 satisfies $\mathcal{P}(\alpha \geq \alpha_0) = q$. Further, the optimal detection threshold on V_y asymptotically approaches $\frac{\alpha_0 P}{2}$ as M gets large.*

Proof. See Appendix A.1. □

Under Rayleigh fading, $f_\alpha(\alpha) = e^{-\alpha}$, $\alpha \geq 0$, and hence, $\mathcal{P}(\alpha \geq \alpha_0) = q$ leads to $e^{-\alpha_0} = q$, or $\alpha_0 = -\log(q)$. Under lognormal shadowing, the cumulative distribution function (cdf) of α is given by $F_\alpha(\alpha) = 1 - Q((\log(\alpha) - \mu_s)/\sigma_s)$, where $Q(\cdot)$ is the standard Gaussian tail function, and μ_s and σ_s are the shape and scale parameters of the shadowing distribution, respectively. Hence, $\alpha_0 = \exp\left(\sigma_s Q^{-1}(q) + \mu_s\right)$. Also, note that the both the error exponent and the detection threshold are independent of π_0, the prior probability of hypothesis $\mathcal{H}_0$, as expected [19, Pg. 389]. Therefore, the error exponent is unaffected by uncertainties in the knowledge of π_0. Conditioned on $\alpha > \alpha_0$, each individual sensor achieves an error exponent of $(\alpha_0 P)^2/8$ on p_f and p_m. An important corollary to the above theorem is that when $q = 1$, under the commonly used fading models such as the Rayleigh, Rician, lognormal, Nakagami distributions, etc., only $\alpha_0 = 0$ solves $\mathcal{P}(\alpha \geq \alpha_0) = 1$, and hence, the error exponent with $q = 1$ is zero.

Another useful aspect of the above theorem is the determination of the asymptotically optimal detection threshold at an individual sensor, $\frac{\alpha_{\min} P}{2}$, where $\alpha_{\min}$ is evaluated in the next section.[6] Due to its asymptotic optimality,the local decision rule of comparing V_y to $\frac{\alpha_{\min} P}{2}$ will be assumed at all sensors in the next section, where the EECL(q) performance at the FC with the OR fusion rule is analyzed.

4. Detection at the fusion center

In this section, we consider an energy-based local decision rule at the individual sensors with the threshold set as $\frac{\alpha_{\min} P}{2}$, where $\alpha_{\min}$ is a parameter to be optimized. We

[6] For the case of a single CR node, $\alpha_{\min} = \alpha_0$.

consider the OR rule for combining the individual decisions at the FC. We use the OR fusion rule because it can detect the presence of the primary signal even if just one of the sensors is not in a deep fade, and also because it possesses an optimality property that we will show later in this section. The main result of this section is stated as the following theorem.

Theorem 2. *When the individual sensors employ energy detection and the FC employs the OR fusion rule, the EECL(q), denoted* $\epsilon_E^{(N)}$*, is given by* $\epsilon_E^{(N)} = \frac{(\alpha_{\min}P)^2}{8}$*, where* $\alpha_{\min}$ *satisfies*

$$\mathcal{P}\left\{\sum_{j=1}^{N}\left(\frac{2\alpha_j}{\alpha_{\min}}-1\right)^2 \mathbb{I}_{\left\{\frac{2\alpha_j}{\alpha_{\min}}>1\right\}} \le 1\right\} = 1-q. \tag{2}$$

In the above, α_j *is the random channel power gain from the primary transmitter to the jth sensor, and* $\mathbb{I}_{\mathcal{A}}$ *is the indicator function, taking value* 1 *when the event* $\mathcal{A}$ *is true and* 0 *otherwise.*

Proof. See Appendix A.2. □

Note that $\alpha_{\min}$ (and hence $\epsilon_E^{(N)}$) increases as N increases. Larger EECL value implies faster decay rates of the corresponding probability of error P_E and hence gives better sensing results. Also, the condition in (2) to determine $\alpha_{\min}$ does not require the fading coefficients from the primary transmitter to the individual sensors to be independent or identically distributed. The joint distribution of the fading coefficients has to be used to evaluate the probability in (2) to find the value of $\alpha_{\min}$, and the solution can be cumbersome to compute in the general case. When the fading coefficients are i.i.d., simpler equations that determine $\alpha_{\min}$ for the cases of Rayleigh fading and lognormal shadowing are stated as the corollary below.

Corollary 1. *When the individual sensors employ energy detection with threshold* $\frac{\alpha_{\min}P}{2}$ *and the FC employs the OR fusion rule, with i.i.d. Rayleigh fading channels between the primary transmitter and the sensors, the EECL(q) is given by* $\frac{(\alpha_{\min}P)^2}{8}$*, where* $\alpha_{\min}$ *satisfies*

$$\left[1-\exp\left(-\frac{\alpha_{\min}}{2}\right)\right]^N + \sum_{l=1}^{N}\binom{N}{l}\left[1-\exp\left(-\frac{\alpha_{\min}}{2}\right)\right]^{N-l}\exp\left(-\frac{\alpha_{\min}}{2}l\right) \times \mathcal{P}\left\{\sum_{k=1}^{l}a_k^2 \le 1\right\} = 1-q. \tag{3}$$

In (3), a_k *is exponentially distributed with parameter* $\frac{2}{\alpha_{\min}}$*. The same detector, under i.i.d. lognormal shadowing, with a threshold of* $\frac{\ell_{\min}P}{2}$ *at the individual sensors, achieves an EECL(q) of* $\frac{(\ell_{\min}P)^2}{8}$*, where* $\ell_{\min}$ *satisfies*

$$P_{\mathcal{A}}^N + \sum_{l=1}^{N}\binom{N}{l}P_{\mathcal{A}}^{N-l}P_{\mathcal{A}^c}^{l}\,\mathcal{P}\left\{\sum_{k=1}^{l}\left(e^{y_k}-1\right)^2 \le 1\right\} = 1-q. \tag{4}$$

Table 1
Values of $\alpha_{\min}$ and $\ell_{\min}$ for different q and N.

N	$q=0.9$		N	$q=0.95$		N	$q=0.99$	
	$\alpha_{\min}$	$\ell_{\min}$		$\alpha_{\min}$	$\ell_{\min}$		$\alpha_{\min}$	$\ell_{\min}$
2	0.39	0.53	2	0.26	0.41	2	0.11	0.26
3	0.66	0.75	3	0.49	0.61	3	0.26	0.41
4	0.88	0.94	4	0.69	0.78	4	0.42	0.55
5	1.07	1.12	5	0.87	0.94	5	0.56	0.68
6	1.24	1.29	6	1.02	1.08	6	0.70	0.79
7	1.39	1.45	7	1.16	1.22	7	0.82	0.91
8	1.52	1.60	8	1.29	1.36	8	0.93	1.01
9	1.65	1.77	9	1.41	1.50	9	1.04	1.12
10	1.76	1.92	10	1.52	1.63	10	1.14	1.23

In (4), y_k *has a truncated Gaussian distribution with mean* $\mu_s + \log\left(\frac{2}{\ell_{\min}}\right)$ *and variance* σ_s^2*, truncated to* $[0,\infty)$*. Also,* $P_{\mathcal{A}^c} \triangleq Q\left(-\frac{\mu_s+\log\left(\frac{2}{\ell_{\min}}\right)}{\sigma_s}\right)$*, and* $P_{\mathcal{A}} \triangleq 1-P_{\mathcal{A}^c}$.

Proof. See Appendix A.3. □

Note that both (3) and (4) need to be numerically solved to obtain $\alpha_{\min}$ and $\ell_{\min}$, respectively. This, in turn, requires the probability terms in the expressions to be evaluated. To this end, we use the simple and tight approximation to the cdf of the sum of Weibull random variates (with parameter $c = 2$) derived in [51] to evaluate the probability term in (3). Also, we use the Pearson type IV distribution approximation in [52] to evaluate the probability term in (4). With this, the values of $\alpha_{\min}$ and $\ell_{\min}$ are very simple to compute; we illustrate the results in Section 6, Table 1.

4.1. Extension to unequal average received signal powers

Recall that, in the above, we had assumed that the CR nodes are sufficiently close to each other that P is the same at all nodes. We now present an extension of our results to handle unequal average received powers at the secondary nodes. First, we consider the case of detection at individual sensors. If the average received power at the ith sensor is P_i, the EECL(q) of that sensor is $(\alpha_{\min}P_i)^2/8$, where $\alpha_{\min}$ is as defined in Theorem 1. Next, for the detection at the fusion center, it is easy to see from the proof of Theorem 2 that the exponent on the false alarm rate is $(\alpha_{\min}P_{\min})^2/8$, where $P_{\min} \triangleq \min_{1\le i\le N} P_i$. The rest of the proof of Theorem 2 also follows through, with P replaced by P_j in (17) and (18) in Appendix A.2. Correspondingly, the condition on $\alpha_{\min}$ in (2) gets modified as:

$$\mathcal{P}\left\{\sum_{j=1}^{N}\left(\frac{P_j}{P_{\min}}\right)^2\left(\frac{2\alpha_j}{\alpha_{\min}}-1\right)^2 \mathbb{I}_{\left\{\frac{2\alpha_j}{\alpha_{\min}}>1\right\}} \le 1\right\} = 1-q. \tag{5}$$

Note that, compared to (2), we have an extra $(P_j/P_{\min})^2$ factor in the summation, since the average received powers are unequal. Hence, with the OR fusion rule, an error exponent of $\epsilon_E^{(N)} = (\alpha_{\min}P_{\min})^2/8$ is achievable, where $\alpha_{\min}$ satisfies the condition in (5).

4.2. Lower bounds on the EECL

In this subsection, we derive lower bounds on $\epsilon_E^{(N)}$ for NB and WB sensing. These lower bounds are easy to calculate and become tight as $q \to 1$. The values obtained from these lower bounds can also be used as a good initialization for solving (3) and (4).

Corollary 2. *In the set-up of Corollary 1, under i.i.d. Rayleigh fading channels, with a threshold of $\frac{\alpha_{\min}^{\mathrm{LB}} P}{2}$ at the individual sensors, a lower bound on the EECL(q) is given by $\frac{(\alpha_{\min}^{\mathrm{LB}} P)^2}{8}$, where $\alpha_{\min}^{\mathrm{LB}}$ satisfies*

$$\alpha_{\min}^{\mathrm{LB}} = 2\left(\frac{1-q}{C_N}\right)^{\frac{1}{N}},$$

$$\text{with } C_N \triangleq \sum_{k=0}^{N} \binom{N}{k} \frac{\pi^{\frac{k}{2}}}{\Gamma\left(1+\frac{k}{2}\right)} \frac{1}{2^k}. \tag{6}$$

Under i.i.d. lognormal shadowing, with a threshold of $\frac{\ell_{\min}^{\mathrm{LB}} P}{2}$ at the individual sensors, a lower bound on the EECL(q) is given by $\frac{(\ell_{\min}^{\mathrm{LB}} P)^2}{8}$, where $\ell_{\min}^{\mathrm{LB}}$ satisfies

$$\ell_{\min}^{\mathrm{LB}} = 2\exp\left(-\sqrt{2\sigma_s^2 \log\left(\frac{1}{\sqrt{2\pi}}\left(\frac{C'_N}{1-q}\right)^{\frac{1}{N}}\right)}\right),$$

$$\text{with } C'_N \triangleq \sum_{k=0}^{N} \binom{N}{k} \frac{\pi^{\frac{k}{2}}}{(2\sigma_s)^k \Gamma\left(1+\frac{k}{2}\right)}. \tag{7}$$

Proof. See Appendix A.4. □

4.3. Optimality of the OR rule

In this subsection, we show that the OR fusion rule satisfies a local optimality property. We show that, when the detection threshold $\frac{\alpha_{\min} P}{2}$ at the individual sensors is chosen to satisfy (2), the OR fusion rule minimizes the probability of error at the FC.

Theorem 3. *For sufficiently large M, the OR fusion rule is probability of error optimal for decentralized detection, when the individual sensors employ energy detection with threshold $\frac{\alpha_{\min} P}{2}$.*

Proof. See Appendix A.5. □

5. Wideband vs. narrowband spectrum sensing

As discussed earlier, when the primary signal is a wideband signal containing a strong pilot tone, spectrum sensing can either be carried out by collecting the signal energy over its entire WB or over a small bandwidth around the pilot [32]. In this section, we characterize the relative performance of these two schemes in terms of the EECL. Let P_{NB} and P_{WB} denote the ratios of the energies of the NB and WB signals to their bandwidths, respectively. Typically, P_{NB} is significantly larger than P_{WB}.

5.1. NB vs. WB sensing at individual sensors

Let ϵ_{NB} and ϵ_{WB} represent the EECL(q) achieved under NB and WB spectrum sensing at a single sensor, respectively. From Section 3, given q, setting $\alpha_0 = -\log q$ and $\ell_0 = \exp(\sigma_s Q^{-1}(q) + \mu_s)$ ensures $\mathcal{P}\{\alpha > \alpha_0\} = \mathcal{P}\{\ell > \ell_0\} = q$. Now, NB sensing outperforms WB sensing in terms of EECL, i.e., $\epsilon_{\mathrm{NB}} > \epsilon_{\mathrm{WB}}$, whenever

$$\left(\frac{P_{\mathrm{NB}}}{P_{\mathrm{WB}}}\right)^2 > \left(\frac{\exp(\sigma_s Q^{-1}(q) + \mu_s)}{-\log q}\right)^2. \tag{8}$$

5.2. NB vs. WB sensing at the fusion center

Similar to the above, let $\epsilon_{\mathrm{NB}}^{(N)}$ and $\epsilon_{\mathrm{WB}}^{(N)}$ represent the EECL(q) achieved by the FC under NB and WB spectrum sensing, respectively. For a given q, $\epsilon_{\mathrm{NB}}^{(N)} > \epsilon_{\mathrm{WB}}^{(N)}$ if $\frac{(\alpha_{\min} P_{\mathrm{NB}})^2}{8} > \frac{(\ell_{\min} P_{\mathrm{WB}})^2}{8}$, i.e., when

$$\left(\frac{P_{\mathrm{NB}}}{P_{\mathrm{WB}}}\right)^2 > \left(\frac{\ell_{\min}}{\alpha_{\min}}\right)^2, \tag{9}$$

where $\alpha_{\min}$ and $\ell_{\min}$ satisfy (3) and (4), respectively.

Note that we have used the Rayleigh fading and the lognormal shadowing assumptions only in evaluating the numerical values of $\alpha_{\min}$ and $\ell_{\min}$ above. That is, the above procedure immediately extends to analyzing the EECL(q) of other fading distributions such as Rician, Nakagamim, Weibull, Suzuki, etc., and the framework can be used to compare NB and WB sensing under various fading conditions.

Also note that, due to the difference in their bandwidths, the sampling rates under NB and WB fading can be different. In the above, we considered the behavior of the sensing performance with respect to M, the number of observations at each sensor. However, the analysis can be easily extended to study the behavior with respect to the sensing duration, as follows. Let $f_{s,\mathrm{NB}}$ and $f_{s,\mathrm{WB}}$ denote the sampling rates of the NB and WB signals, respectively. Then, a given spectrum sensing duration of T_{ss} leads to a probability of error approximately given by $P_{E,NB} \triangleq \exp(-T_{\mathrm{ss}} f_{s,\mathrm{NB}} \epsilon_{\mathrm{NB}})$ and $P_{E,\mathrm{WB}} \triangleq \exp(-T_{\mathrm{ss}} f_{s,\mathrm{WB}} \epsilon_{\mathrm{WB}})$ in the two cases.

Suppose $f_{s,\mathrm{WB}} = B f_{s,\mathrm{NB}}$, where B is the ratio of bandwidths of the WB and NB signals. Thus, NB detection outperforms WB detection in terms of the EECL with the same confidence q and when both detectors sense for the same duration, if

$$\frac{(\alpha_{\min} P_{\mathrm{NB}})^2}{8} > B\frac{(\ell_{\min} P_{\mathrm{WB}})^2}{8}. \tag{10}$$

For a given signal bandwidth, as B is increased (i.e., as the bandwidth of the NB signal is decreased), P_{NB} also increases relative to P_{WB}, since the NB filter captures the energy in the pilot tone more accurately. If the NB signal consists of a pure pilot tone, the ratio $\frac{P_{\mathrm{NB}}}{P_{\mathrm{WB}}}$ increases linearly with B. Thus, by using a large enough B, NB sensing can be made to outperform WB sensing for a given sensing duration, since the factor B appears quadratically in the

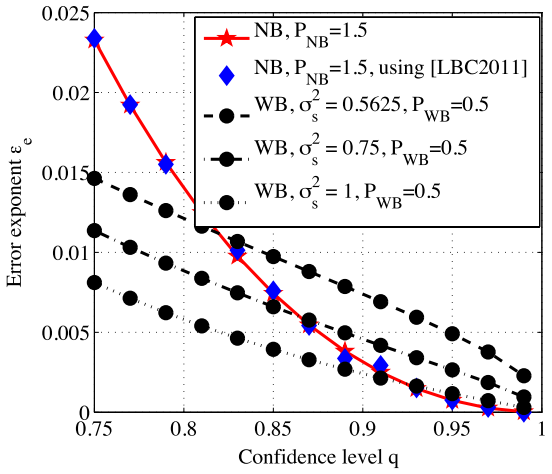

Fig. 2. Trade-off between NB and WB sensing at a single sensor, with $\mu_s = 0$ in the WB case.

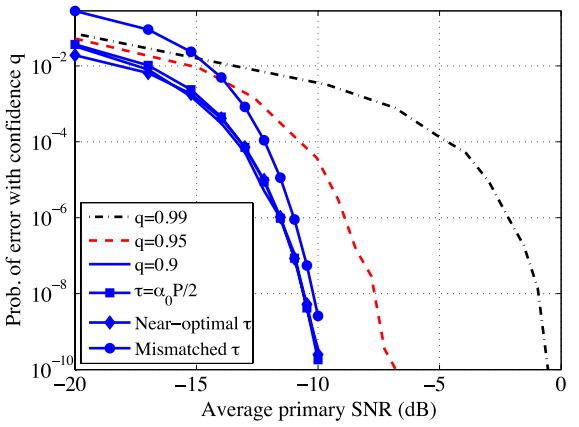

Fig. 3. Variation of p_e with a confidence q at a single sensor as a function of SNR, under narrowband Rayleigh fading. Here, $N = 1$, $\pi_0 = 0.5$, $M = 10^6$. The curve labeled '`Mismatched` τ' corresponds to using $\pi_0 = 0.5$ to design the detector, when the actual $\pi_0 = 0.01$.

error exponent term, while it occurs only linearly in the detection delay term. However, increasing B comes at the cost of an increasing accuracy in the CR's knowledge of the frequency of the pilot tone in the primary signal.

6. Numerical results and simulations

In this section, we present simulation results to validate the analytical development in the preceding sections, and to illustrate the relative performance of NB and WB sensing schemes. For the NB and WB cases, we denote the signal powers by P_{NB} and P_{WB}, and we let the channel gains be Rayleigh distributed and lognormal distributed, respectively. The prior probability was chosen to be $\pi_0 = 0.5$ for all the simulations. For comparison with existing results, we extend the analysis in [14] to derive the probability of error with a confidence level, and then calculate the EECL(q) from it. We also compare the performance of our detector with the detector designed under the NP criterion [32], for both NB and WB cases, as well as for single sensor detection and decentralized detection with multiple sensors.

6.1. Detection at the sensors

In Fig. 2, we plot EECL(q) as a function of the confidence level q, for the NB and WB fading models, with $\frac{P_{\text{NB}}}{P_{\text{WB}}} = 3$. In the WB fading case, we show the curves for three typical values of the shadowing parameter σ_s^2. First, note that all the curves approach an EECL of 0 as q approaches 1, i.e., the conventional error exponent is zero under both NB and WB fading, as expected. As the confidence level is decreased, the NB sensing outperforms the WB sensing. Also, in the single sensor case, the design in [14] (denoted by [LBC2011] in the legend) corresponds to using an NB detector. The excellent match between our results and those derived from [14] is clear from the plot.

Next, we simulated the probability of error with confidence $q = 0.9$ at very low error probabilities, using importance sampling [53]. Fig. 3 shows the performance as a function of the average primary SNR, for various values of q. The waterfall-type behavior of the curve indicates a positive error exponent with a confidence level under fading. Also, as mentioned earlier, an advantage of the error exponent approach is that the threshold, $\tau = \frac{\alpha_0 P}{2}$, is independent of the prior probability π_0. In the figure, we see that the performance with $\tau = \frac{\alpha_0 P}{2}$ matches well with that obtained by using the near-optimal threshold derived in [30]. We illustrate the effect of mismatched π_0 in Fig. 3. The performance loss due to lack of knowledge of π_0 is over 3 dB at a probability of error of 10^{-2}, when $M = 10^6$. For lower values of M, the performance loss would be much higher, because of the inverse square-root relationship between the number of samples and the SNR required to achieve a given performance [30].

6.2. Detection at the fusion center

We now consider the decentralized set-up with the OR fusion rule for combining the individual decisions from N sensors. In Fig. 4, we show the variation of the lower bound on $\epsilon_E^{(N)}$ with confidence $q = 0.99$. The detection threshold parameters $\alpha_{\min}^{\text{LB}}$ and $\ell_{\min}^{\text{LB}}$ are obtained from (6) and (7). We see that the lower bound closely approximates the cross-over behavior of the NB and WB sensing schemes, shown in Fig. 5. For obtaining the latter curve, the detection thresholds are found by numerically solving (3) and (4) for the NB and WB cases, respectively.

We plot $\epsilon_E^{(N)}$ as a function of the power ratio $\frac{P_{\text{NB}}}{P_{\text{WB}}}$ in Fig. 6, for different values of q, and with $N = 4$. Both Figs. 5 and 6 show the cross-over between NB and WB sensing: as $\frac{P_{\text{NB}}}{P_{\text{WB}}}$ is increased, NB sensing outperforms WB sensing. Next, the variation of $\epsilon_E^{(N)}$ with the number of sensors N is shown in Fig. 7, with the power ratio $\frac{P_{\text{NB}}}{P_{\text{WB}}} = 1$. The plot shows an approximately linear improvement in the EECL(q) as the number of sensors is increased.

Next, we present simulation results of the probability of error at the FC, P_E, with the signal modeled as the sum of a sinusoidal component and an AWGN component, varying

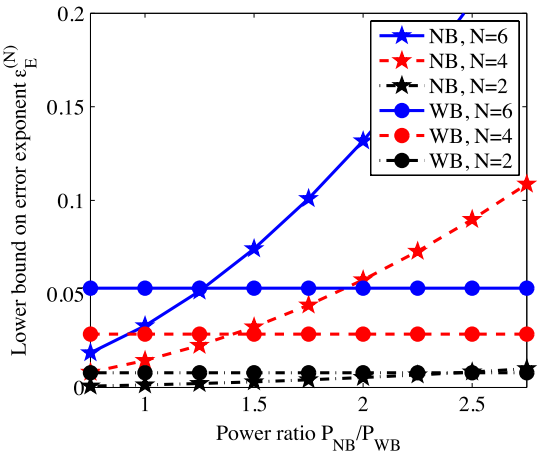

Fig. 4. Comparison of NB and WB sensing at the fusion center in terms of the lower bound on $\epsilon_E^{(N)}$, with $q = 0.99$, $\mu_s = 0$, $\sigma_s = 1$. The cross-over points between NB and WB sensing closely match with the corresponding cross-over points of the EECL in Fig. 5.

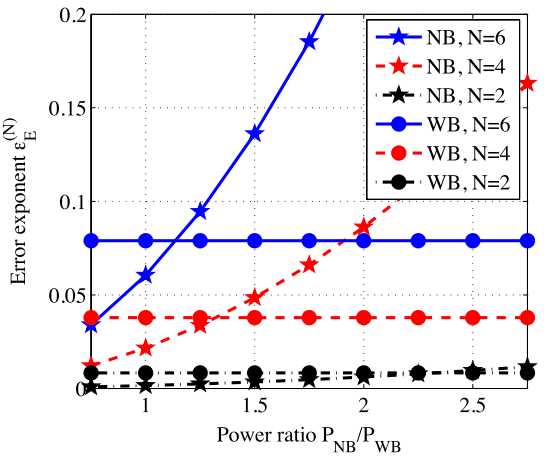

Fig. 5. Comparison of NB and WB sensing at the fusion center in terms of the EECL $\epsilon_E^{(N)}$, with $q = 0.99$, $\mu_s = 0$, $\sigma_s = 1$. Note the improvement in EECL with increasing N.

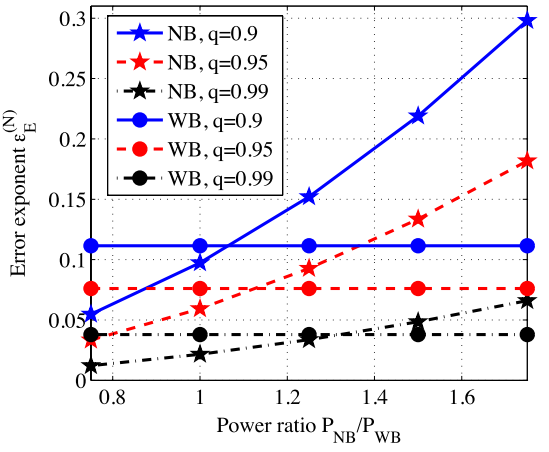

Fig. 6. Illustration of the comparison of NB and WB sensing at the fusion center in terms of $\epsilon_E^{(N)}$, with $N = 4$, $\mu_s = 0$, $\sigma_s = 1$, and for different values of q.

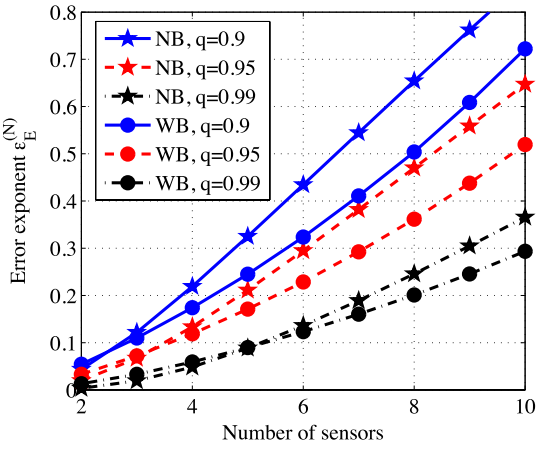

Fig. 7. Illustration of the improvement in $\epsilon_E^{(N)}$ as a function of N, the number of sensors, with $\frac{P_{NB}}{P_{WB}} = 1$, $\mu_s = 0$, $\sigma_s = 1$. As N gets sufficiently large, NB sensing outperforms WB sensing.

ratio of their powers according to $\frac{P_{NB}}{P_{WB}}$. The bandwidths of the NB and WB signals are fixed as 1 kHz and 20 kHz, respectively. The sensing duration is chosen as 20 ms. We compute the probability of error with confidence q by computing the probability of error for 1000 i.i.d. channel states, and discounting a fraction $1-q$ of the channel states that yield the highest probability of miss when averaged over 10,000 noise instantiations. Under this set-up, we plot the probability of error with $N = 2, 4, 6$ and confidence level $q = 0.99$ in Figs. 8 and 9. From Fig. 8, we see that the power ratio at which the cross-over between NB and WB sensing occurs is roughly the same as the cross-over points in the EECL plot of Fig. 5, i.e., the EECL does capture the probability of error behavior of the detectors. In Fig. 9, we compare the performance of our design with that of the NP-based design adopted in [32,38], for both single-sensor detection and decentralized detection, and for both the NB and WB cases. The NP test is designed to meet a false alarm probability target of 0.01. We see that, while the probability of error with confidence $q = 0.99$ of the NP test saturates as the average primary SNR increases, the performance of our EECL-based design exhibits a waterfall-type drop with increasing SNR. Note that, for the settings in this simulation, the EECL of NB sensing is higher than that of WB sensing. Since having a larger average primary SNR is akin to having a larger number of observations at the individual sensors, one would expect that NB sensing should outperform WB sensing as the average primary SNR increases; this is also corroborated by Fig. 9.

Finally, Table 1 shows the values of $\alpha_{\min}$ and $\ell_{\min}$ for different q and N. It can be seen that both $\alpha_{\min}$ and $\ell_{\min}$ increase with N and decrease with q. Using importance sampling, the theoretical and experimental values of the error exponents obtained for different values of P, q and N are listed in Tables 2 and 3. We note the good agreement between the theoretical and simulated error exponents, even at very low exponent values.

Table 2
EECL(q) at a single sensor, with $N = 1$ and Rayleigh fading. All values have to be multiplied by 10^{-5}.

P (dB)	$q = 0.9$		P (dB)	$q = 0.95$		P (dB)	$q = 0.99$	
	Th	Sims		Th	Sims		Th	Sims
−10	1.39	2.20	−2.25	11.84	14.28	0	1.26	2.32
−7	5.55	6.57	−1.5	16.11	17.64	2	2.84	4.39
−5	12.49	13.63	−1	21.05	22.30	3	5.05	7.34
−4	22.02	23.56	−0.5	26.66	28.23	4	7.89	9.36
−3	34.69	35.91	0	32.89	34.19	5	11.36	14.49

Table 3
EECL(q) at the FC, with $P = -10$ dB and Rayleigh fading. All values have to be multiplied by 10^{-4}.

N	$q = 0.9$		N	$q = 0.95$	
	Th	Sims		Th	Sims
2	1.94	2.11	2	0.87	0.88
3	5.41	6.12	3	2.97	3.52
4	9.73	10.28	4	5.93	6.34

Table 4
EECL(q) at the FC, with $N = 4, P = -10$ dB, i.i.d. Rayleigh fading in the NB case and geometrically correlated lognormal shadowing in the WB case. All values have to be multiplied by 10^{-4}.

ρ_{cor}	$q = 0.9$		$q = 0.95$	
	$\epsilon_{NB}^{(N)}$	$\epsilon_{WB}^{(N)}$	$\epsilon_{NB}^{(N)}$	$\epsilon_{WB}^{(N)}$
0	10.28	8.95	7.60	6.14
0.25	–	4.07	–	5.64
0.5	–	3.77	–	3.23
0.75	–	3.61	–	2.70

As mentioned earlier, we assume that the channels from PU to CR nodes undergo i.i.d. fading. Even if the sensors were close together, it is reasonable to assume that the Rayleigh fading components are independent. However, the nodes in the WB sensing case may undergo correlated lognormal shadow fading. Table 4 illustrates the performance of WB vs. NB sensing with geometrically correlated lognormal shadowing. It can be seen that, as the correlation increases, the EECL of the WB case drops. Hence, in the cases where NB scheme outperforms the WB scheme in the absence of channel correlation, it continues to outperform the WB scheme even for nonzero correlation values.

The performance of any distributed detection scheme would degrade in presence of reporting channel errors, but this may not impact the fundamental tradeoff between WB and NB detection schemes. To illustrate this, simulation results with noisy reporting channels is presented in Table 5. The channel between the individual sensors and the FC is modeled as a binary symmetric channel with error probability $e_{\mathtt{bsc}}$. It can be observed that the relative performance of WB and NB sensing schemes is retained even when the reporting channels are noisy. As the channel error rate increases, the reporting channel errors dominate the performance, and, consequently, the EECL approaches the same constant value in both cases, as expected.

7. Conclusions

In this paper, we analyzed the performance of energy-based Bayesian decentralized detection for spectrum sensing in cognitive radios, with the exponent on the probability of error as the performance metric. We introduced a novel performance metric called the Error Exponent with a Confidence Level (EECL), and derived the EECL at a given confidence level $q < 1$. We used the EECL to answer the question of whether it is better to sense for the pilot tone in a narrow band, or to sense the entire wide-band signal.

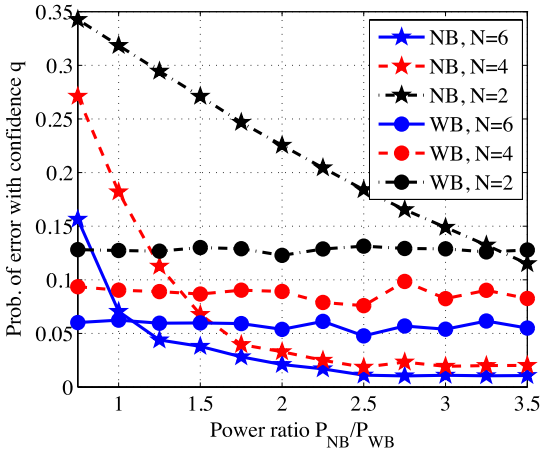

Fig. 8. Variation of the probability of error with a confidence level at the fusion center with $\frac{P_{NB}}{P_{WB}}$, for $q = 0.99$, $\mu_s = 0$, $\sigma_s = 1$ and $\pi_0 = 0.5$. The cross-over of the probability of error between NB and WB sensing occurs at roughly the same $\frac{P_{NB}}{P_{WB}}$ ratio as in the EECL plots.

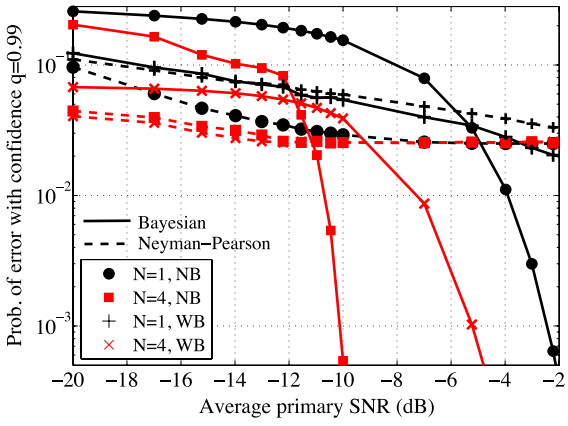

Fig. 9. Comparison of the Bayesian, EECL based design considered in this paper (curves labeled `Bayesian`) and Neyman–Pearson approach in [32,38] (curves labeled `Neyman-Pearson`), in terms of the P_E with a confidence $q = 0.99$, as a function of the average primary SNR, with $\mu_s = 0, \sigma_s = 1$ and $\pi_0 = 0.5$. The EECL based design shows a waterfall-type behavior due to the positive error exponent, while the conventional NP based design exhibits an error floor.

Table 5
EECL(q) at the FC, with $N = 4$, $P = -10$ dB and the link between each sensor and FC is modeled as BSC with error probability e_{bsc}. All values have to be multiplied by 10^{-4}.

e_{bsc}	$q = 0.9$		$q = 0.95$	
	$\epsilon_{NB}^{(N)}$	$\epsilon_{WB}^{(N)}$	$\epsilon_{NB}^{(N)}$	$\epsilon_{WB}^{(N)}$
0.0001	9.25	9.16	6.90	7.19
0.001	7.1	6.91	6.11	6.91
0.01	0.46	0.46	0.23	0.23

We also derived simplified expressions for finding the detection threshold and the EECL for the i.i.d. Rayleigh fading and lognormal shadowing cases. We validated the theoretical expressions through simulations. Future work could include incorporating correlation in the signal or noise, extending the results to allow for time-varying channels, and optimally combining NB and WB spectrum sensing.

Acknowledgment

The first author would like to thank Srinivas Reddy for discussions on importance sampling.

Appendix

A.1. Proof of Theorem 1

It is straightforward to show that the likelihood ratio test corresponding to (1) is monotonically increasing in V_y (by examining the derivatives of the likelihood ratio with respect to V_y), and hence, the optimum test reduces to a threshold test on V_y itself. That is, it declares H_1 when $V_y \geq x$, where x is the detection threshold. Let $f_\alpha(\alpha)$ denote the pdf of α. Conditioned on $\mathcal{A} \triangleq \{\alpha \geq \alpha_0\}$, the pdf of α is $f_{\alpha|\mathcal{A}}(\alpha|\mathcal{A}) = f_\alpha(\alpha)/\mathcal{P}(\mathcal{A}), \alpha \geq \alpha_0$. By construction, $\mathcal{P}(\mathcal{A}) = q$. The probability of error is given by

$$p_e = \pi_0 Q(x\sqrt{M}) + \pi_1 \int_{-\infty}^{x}\int_{\alpha_0}^{\infty} f_{\mathcal{N}}\left(v - \alpha P, \frac{1}{\sqrt{M}}\right) \times \frac{f_\alpha(\alpha)}{q} \mathrm{d}\alpha \mathrm{d}v, \tag{11}$$

where $f_{\mathcal{N}}(x, \sigma)$ is the Gaussian pdf with mean zero and variance σ^2 evaluated at x, $\pi_0 \triangleq \mathcal{P}(H_0)$, and $\pi_1 \triangleq \mathcal{P}(H_1) = 1 - \pi_0$. To find the optimum threshold, we differentiate the above w.r.t. x and equate to 0. After some simplification, we get

$$\frac{q\pi_0}{\pi_1} = \int_{\alpha_0}^{\infty} \exp\left(M\left(x\alpha P - \frac{\alpha^2 P^2}{2}\right)\right) f_\alpha(\alpha)\mathrm{d}\alpha. \tag{12}$$

Let x_M denote the solution to the above equation for a given value of M.[7] First, we show that x_M converges to $\alpha_0 P/2$. To do this, we show that neither $x_M < \alpha_0 P/2$ nor $x_M > \alpha_0 P/2$ are possible for large M, as they lead to a contradiction. Define $g(x, \alpha) \triangleq x\alpha P - \alpha^2 P^2/2$. Note that $g(\alpha_0 P/2, \alpha) \leq 0$ for $\alpha \geq \alpha_0$. If $x_M < \alpha_0 P/2$, since $g(x, \alpha)$ is monotonic in x, we have $g(x_M, \alpha) < 0$ for $\alpha \geq \alpha_0$. Let $g_{\max} \triangleq \max_{\alpha \geq \alpha_0} g(x_M, \alpha)$, and note that $g_{\max} < 0$. Then, using $g_{\max} \geq g(x_M, \alpha)$ in (12) results in the following upper bound on the right hand side (RHS): RHS $\leq \exp(Mg_{\max}) \int_{\alpha_0}^{\infty} f_\alpha(\alpha)\mathrm{d}\alpha$. Since $g_{\max} < 0$, the upper bound can be made as small as desired by choosing M sufficiently large. Thus, if $x_M < \alpha_0 P/2$, the right hand side goes to zero as M gets large, and hence, attaining equality in (12) is not possible. Hence, x_M must satisfy $x_M \geq \alpha_0 P/2$.

Next, we show that $x_M \geq x_0 > \alpha_0 P/2$ also leads to a contradiction. Consider α such that $g(x_0, \alpha) > 0$. This corresponds to $\alpha < 2x_0/P$. By the assumption, we have $\alpha_0 < 2x_0/P$, so that, $g(x_0, \alpha) > 0$ for $\alpha_0 \leq \alpha < 2x_0/P$. Further, if $g(x_0, \alpha) > 0$ and $x_M \geq x_0$, we have $g(x_M, \alpha) > 0$. Therefore, there exists an $\epsilon > 0$ such that $g(x_M, \alpha) > 0$ for $\alpha_0 \leq \alpha \leq 2x_0/P - \epsilon$. Let $g_{\min} \triangleq \min_{\alpha \in [\alpha_0, 2x_0/P - \epsilon]} g(x_M, \alpha)$, and note that $g_{\min} > 0$. Then, the right hand side in (12) can be lower bounded as

$$\text{RHS} \geq \int_{\alpha_0}^{\frac{2x_0}{P} - \epsilon} \exp\left(Mg(x_M, \alpha)\right) f_\alpha(\alpha)\mathrm{d}\alpha \tag{13}$$

$$\geq \exp\left(Mg_{\min}\right) \int_{\alpha_0}^{\frac{2x_0}{P} - \epsilon} f_\alpha(\alpha)\mathrm{d}\alpha. \tag{14}$$

Since $g_{\min} > 0$, the above lower bound can be made as large as desired by choosing M sufficiently large, since the integral term is a strictly positive constant. This implies that if $x_M \geq x_0 > \alpha_0 P/2$, the right hand side grows unbounded as M gets large, and hence, attaining equality in (12) is not possible. Hence, x_M converges to $\alpha_0 P/2$ as M goes to infinity.

Now, consider the exponent due to the false alarm term. This is simply given by

$$\epsilon_f \triangleq \lim_{M \to \infty} \frac{-\log\left(Q(x_M\sqrt{M})\right)}{M} = \frac{\alpha_0^2 P^2}{8}. \tag{15}$$

In the above, $Q(y)$ is the standard Gaussian tail probability evaluated at y. The second equality above is obtained by upper and lower bounding $Q(y)$ for large y and showing that both limits equal as $M \to \infty$. Since the exponents due to the false alarm and the missed detection are equal in a Bayesian set-up [19, Chap. 11], [23], it follows that the EECL(q) on the probability of error is $\frac{\alpha_0^2 P^2}{8}$, where α_0 is chosen to satisfy $\mathcal{P}(\alpha > \alpha_0) = q$.

A.2. Proof of Theorem 2

Suppose that the hypothesis $\mathcal{H}_0$ is true. With the OR fusion rule, a false alarm at any of the sensors results in a false alarm at the FC. Since, conditioned on $\mathcal{H}_0$, the sensor decisions are independent, the false alarm probability at the FC, denoted by P_F, is simply $1-(1-p_f)^N$, where p_f is the false alarm probability at an individual sensor. Now, given the detection threshold $\frac{\alpha_{\min} P}{2}$ at the sensors, the exponent ϵ_F at the FC is determined by the p_f term in the expansion of $1 - (1 - p_f)^N$. Thus, the error exponent at the FC is the same as that at the individual sensors, i.e., $\epsilon_F = \frac{(\alpha_{\min} P)^2}{8}$.

Suppose that the hypothesis $\mathcal{H}_1$ is true. Conditioned on α_j, the channel power gain from the primary transmitter to sensor j, the decision statistic V_y at the jth sensor is

[7] That a unique solution exists can be seen from simple monotonicity arguments.

distributed as $\mathcal{N}\left(\alpha_j P, \frac{1}{M}\right)$. Since the jth sensor uses a threshold of $\frac{\alpha_{\min} P}{2}$ for detection, using well-known bounds on the Q-function,[8] it is easy to show that the missed detection probability at the jth sensor conditioned on α_j, denoted $p_{m_j|\alpha_j}$, is given by

$$\begin{aligned} p_{m_j|\alpha_j} &= \mathcal{P}\left\{ V_y < \frac{\alpha_{\min} P}{2} \middle| \alpha_j \right\} \\ &= Q\left(\sqrt{M}\left(\frac{\alpha_{\min} P}{2} - \alpha_j P\right)\right) \\ &\doteq \exp\left(-\frac{M}{2}\left(\alpha_j P - \frac{\alpha_{\min} P}{2}\right)^2 \mathbb{I}_{\left\{\alpha_j > \frac{\alpha_{\min}}{2}\right\}}\right) \end{aligned} \tag{16}$$

where the notation $f(M) \doteq \exp(-M\beta)$ is used to mean $\lim_{M\to\infty} \frac{-\log f(M)}{M} = \beta$. That is, the jth sensor achieves an error exponent of $\frac{1}{2}\left(\alpha_j P - \frac{\alpha_{\min} P}{2}\right)^2$ if $\alpha_j > \frac{\alpha_{\min} P}{2}$, and zero otherwise.

With the OR fusion rule, when hypothesis $\mathcal{H}_1$ is true, the FC makes an error and declares $\mathcal{H}_0$ only if all the sensors make an error. Hence, given $\alpha_1, \ldots, \alpha_N$, the missed detection probability at the FC $P_{M|\alpha_1,\ldots,\alpha_N}$ is given by

$$\begin{aligned} P_{M|\alpha_1,\ldots,\alpha_N} &= \prod_{j=1}^{N} p_{m_j} \\ &\doteq \exp\left(-\frac{M}{2}\sum_{j=1}^{N}\left(\alpha_j P - \frac{\alpha_{\min} P}{2}\right)^2 \mathbb{I}_{\left\{\alpha_j > \frac{\alpha_{\min}}{2}\right\}}\right). \end{aligned} \tag{17}$$

Now consider the case where $\alpha_1, \alpha_2, \ldots, \alpha_N$ are random. The FC attains an EECL(q) of ϵ_M, provided

$$\begin{aligned} &\mathcal{P}\left\{\frac{1}{2}\sum_{j=1}^{N}\left(\alpha_j P - \frac{\alpha_{\min} P}{2}\right)^2 \mathbb{I}_{\left\{\alpha_j > \frac{\alpha_{\min}}{2}\right\}} \le \epsilon_M\right\} \\ &\le 1 - q, \end{aligned} \tag{18}$$

where the probability is taken over the distribution of $\alpha_1, \alpha_2, \ldots, \alpha_N$. The best error exponent is obtained, i.e., ϵ_M is maximized, when the left hand side above equals $1 - q$, since, otherwise, ϵ_M (and $\alpha_{\min}$) can be increased to improve the error exponent.

Finally, for optimal Bayesian detection, the exponent associated with the false alarm and missed detection must be equal, i.e., $\epsilon_F = \epsilon_M$ [19, Chap. 11], [23]. Hence, substituting $\epsilon_M = \frac{(\alpha_{\min} P)^2}{8}$ in (18) and simplifying, we get (2), which completes the proof.

A.3. Proof of Corollary 1

Let $\alpha_{\min}$ and $\ell_{\min}$ denote the solution to (2) under the Rayleigh fading and lognormal shadowing cases, respectively. Let $\texttt{expn}(\lambda)$ and $\texttt{LN}(\mu, \sigma)$ denote the exponential distribution with parameter λ and the lognormal distribution with parameters μ and σ, respectively. Now, under Rayleigh fading, $t_j \triangleq \frac{2\alpha_j}{\alpha_{\min}} \sim \texttt{expn}\left(\frac{2}{\alpha_{\min}}\right)$, while under lognormal shadowing, with a slight abuse of notation, $t_j \triangleq \frac{2\alpha_j}{\ell_{\min}} \sim \texttt{LN}\left(\mu_s + \log\left(\frac{2}{\ell_{\min}}\right), \sigma_s\right)$. Let $Z \triangleq \sum_{j=1}^{N}\left(t_j - 1\right)^2 \mathbb{I}_{\{(t_j-1)\ge 0\}}$, for notational convenience. From Theorem 2, note that we need to find $\alpha_{\min}$ such that $F_Z(1) = 1 - q$, where $F_Z(\cdot)$ is the CDF of Z.

$$\begin{aligned} &\mathcal{P}\{Z \le 1\} \\ &= \sum_{l=0}^{N} \mathcal{P}\{l \text{ out of } N\ t_j\text{'s are } \ge 1\} \\ &\quad \times \mathcal{P}\{Z \le 1 | l \text{ out of } N\ t_j\text{'s are } \ge 1\} \\ &= \sum_{l=1}^{N}\binom{N}{l}\left(\mathcal{P}\left\{t_j \le 1\right\}\right)^{N-l}\left(\mathcal{P}\left\{t_j > 1\right\}\right)^{l} \\ &\quad \times \mathcal{P}\left\{\sum_{k=1}^{l}\left(t_k - 1\right)^2 \le 1 \middle| t_k > 1, k = 1, \ldots, l\right\} \\ &\quad + \left(\mathcal{P}\left\{t_k \le 1\right\}\right)^N, \end{aligned} \tag{19}$$

which should equal $1 - q$ by requirement, with $t_k \sim \texttt{expn}\left(\frac{2}{\alpha_{\min}}\right)$ for Rayleigh fading, and $t_k \sim \texttt{LN}\left(\mu_s + \log\left(\frac{2}{\ell_{\min}}\right), \sigma_s\right)$, for the shadowing, respectively. In the Rayleigh fading case, by the memoryless property of exponential random variables, it is easy to show that

$$\begin{aligned} &\mathcal{P}\left\{\sum_{k=1}^{l}\left(t_k - 1\right)^2 \le 1 \middle| t_k > 1, k = 1, \ldots, l\right\} \\ &= \mathcal{P}\left\{\sum_{k=1}^{l} a_k^2 \le 1\right\}, \end{aligned} \tag{20}$$

where $a_k \sim \texttt{expn}\left(\frac{2}{\alpha_{\min}}\right)$ are independent and exponentially distributed. Since $\mathcal{P}\left\{t_k > 1\right\} = e^{-\frac{2}{\alpha_{\min}}}$, (19) reduces to the expression in (3).

The proof for the lognormal shadowing case is similar to the Rayleigh fading case, and follows by noting that $\mathcal{P}\left\{t_k \le 1\right\} = \mathcal{P}\left\{\log t_k \le 0\right\} = Q\left(\frac{\mu_s + \log\left(\frac{2}{\ell_{\min}}\right)}{\sigma_s}\right)$. Further,

$$\begin{aligned} &\mathcal{P}\left\{\sum_{k=1}^{l}\left(t_k - 1\right)^2 \le 1 \middle| t_k > 1, k = 1, \ldots, l\right\} \\ &= \mathcal{P}\left\{\sum_{k=1}^{l}\left(e^{y_k} - 1\right)^2 \le 1\right\}. \end{aligned} \tag{21}$$

In the above, $y_k \triangleq \log t_k$, and, due to the conditioning on $t_k > 1$, we have that y_k has a truncated Gaussian distribution, with pdf $\frac{\mathcal{N}\left(\mu_s + \log\left(\frac{2}{\ell_{\min}}\right), \sigma_s^2\right)}{Q\left(-\frac{\mu_s + \log\left(\frac{2}{\ell_{\min}}\right)}{\sigma_s}\right)}$ for $y_k > 0$ and zero otherwise.

A.4. Proof of Corollary 2

Consider the left hand side of (3). Upper bounding the terms in the expression would lead to a lower bound on $\alpha_{\min}$, and, consequently, on the EECL(q). First, note that $1 - \exp\left(\frac{\alpha_{\min}}{2}\right) \le \frac{\alpha_{\min}}{2}$. Also, a_k in (3) is distributed as $f_{a_k}(a_k) = \frac{\alpha_{\min}}{2}\exp\left(-\frac{\alpha_{\min} a_k}{2}\right)$, $a_k \ge 0$, and hence, $f_{a_k}(a_k) \le \frac{\alpha_{\min}}{2}$. Thus, by replacing the pdf of a_k with its upper bound, we get

[8] For example, $\frac{y}{1+y^2}\frac{1}{\sqrt{2\pi}}e^{-\frac{y^2}{2}} \le Q(y) \le \frac{1}{y\sqrt{2\pi}}e^{-\frac{y^2}{2}}$.

$$\mathcal{P}\left(\sum_{k=1}^{l} a_k^2 \le 1\right) = \int_{\sum_{k=1}^{l} a_k^2 \le 1, a_k \ge 0} f_{a_k}(a_1) f_{a_k}(a_2) \cdots f_{a_k}(a_l) \mathrm{d}a_1 \mathrm{d}a_2 \cdots \mathrm{d}a_l \le \left(\frac{\alpha_{\min}}{2}\right)^l \int_{\sum_{k=1}^{l} a_k^2 \le 1, a_k \ge 0} \mathrm{d}a_1 \mathrm{d}a_2 \cdots \mathrm{d}a_l = \left(\frac{\alpha_{\min}}{2}\right)^l \frac{\mathcal{V}_l}{2^l}, \quad (22)$$

where $\mathcal{V}_l = \frac{\pi^{\frac{k}{2}}}{\Gamma\left(1+\frac{k}{2}\right)}$ is the volume of the l-dimensional unit sphere, with $\Gamma(\cdot)$ being the Gamma function. The 2^l factor in the denominator arises because only the volume of the first orthant is relevant here, since $a_k \ge 0$. Substituting in (3), we get a lower bound on $\alpha_{\min}$ by solving

$$\left(\frac{\alpha_{\min}^{\mathrm{LB}}}{2}\right)^N + \sum_{l=1}^{N} \binom{N}{l} \left(\frac{\alpha_{\min}^{\mathrm{LB}}}{2}\right)^{N-l} \left(\frac{\alpha_{\min}^{\mathrm{LB}}}{2}\right)^l \frac{\mathcal{V}_l}{2^l} = 1 - q. \quad (23)$$

The result in (6) follows from rearranging the above equation.

The proof for the lognormal shadowing case is similar. Starting from (4), using a well-known bound on the Q-function, we upper bound $P_{\mathcal{A}}$ as

$$P_{\mathcal{A}} \le \frac{1}{\sqrt{2\pi}} \exp\left(-\frac{\left(\log\left(\frac{2}{\ell_{\min}}\right)\right)^2}{2\sigma_s^2}\right). \quad (24)$$

Next, conditioned on $y_k > 0$, it is easy to show that $z_k \triangleq e^{y_k} - 1$ is distributed as

$$f_{z_k}(z_k) = \frac{1}{(z_k+1)\sigma_s\sqrt{2\pi}} \times \frac{\exp\left(-\frac{(\log(z_k+1)-\log(2/\ell_{\min}))^2}{2\sigma_s^2}\right)}{Q\left(\frac{-\log(2/\ell_{\min})}{\sigma_s}\right)}, \quad z_k \ge 0. \quad (25)$$

Further, since $\ell_{\min} \le 1$, setting $z_k = 0$ in the right hand side above leads to an upper bound on $f_{z_k}(z_k)$. Hence, we have

$$\mathcal{P}\left(\sum_{k=1}^{l} z_k^2 \le 1\right) \le \left(\frac{1}{\sigma_s\sqrt{2\pi}} \frac{\exp\left(-\frac{(\log(2/\ell_{\min}))^2}{2\sigma_s^2}\right)}{Q\left(-\frac{\log(2/\ell_{\min})}{\sigma_s}\right)}\right)^l \frac{\mathcal{V}_l}{2^l}. \quad (26)$$

Substituting the upper bounds in (24) and (26) into (4), and using the fact that $P_{\mathcal{A}^c} = Q\left(-\frac{\log(2/\ell_{\min})}{\sigma_s}\right)$, and simplifying, we get the result in (7).

A.5. Proof of Theorem 3

It is known that, with conditionally i.i.d. observations at the sensors, the probability of error at the FC is minimized by the K out of N rule, and the optimum K is given by [48]

$$K_{opt} = \min\left(N, \left\lceil \frac{\log\left(\frac{\pi_0}{1-\pi_0}\right) + N\log\left(\frac{1-p_f}{p_m}\right)}{\log\left\{\left(\frac{1-p_m}{p_f}\right)\left(\frac{1-p_f}{p_m}\right)\right\}} \right\rceil\right), \quad (27)$$

where p_f and p_m are the false alarm and missed detection probabilities, respectively, at the individual nodes. Now, given the detection threshold $\frac{\alpha_{\min}P}{2} > 0$ at the individual sensors, p_f clearly decreases with an exponent $\frac{(\alpha_{\min}P)^2}{8}$. On the other hand, whenever $\alpha < \alpha_{\min}$, the missed detection probability of the hypothesis test in (1) is lower bounded by $\frac{1}{2}$. Since the event $\alpha < \alpha_{\min}$ occurs with a nonzero probability, the exponent on p_m is 0. Thus,

$$\left\lceil \frac{\log\left(\frac{\pi_0}{1-\pi_0}\right) + N\log\left(\frac{1-p_f}{p_m}\right)}{\log\left\{\left(\frac{1-p_m}{p_f}\right)\left(\frac{1-p_f}{p_m}\right)\right\}} \right\rceil \to 1, \quad (28)$$

since the numerator approaches a constant, while the denominator is linearly increasing with M. Thus, for sufficiently large M, $K_{opt} = 1$, i.e., the OR fusion rule is optimal.

References

[1] J. Mitola III, Cognitive radio: An integrated agent architecture for software defined radio (Ph.D. thesis), Royal Institute of Technology (KTH), Sweden, 2000.
[2] E. Visotsky, S. Kuffner, R. Peterson, On collaborative detection of TV transmissions in support of dynamic spectrum sharing, in: Proc. DySPAN, pp. 338–345.
[3] J. Unnikrishnan, V. Veeravalli, Cooperative sensing for primary detection in cognitive radio, IEEE J. Sel. Top. Sign. Proces. 2 (2008) 18–27.
[4] I.F. Akyildiz, B.F. Lo, R. Balakrishnan, Cooperative spectrum sensing in cognitive radio networks: A survey, Phys. Commun. 4 (2011) 40–62.
[5] Y.-C. Liang, K.-C. Chen, G. Li, P. Mahonen, Cognitive radio networking and communications: an overview, IEEE Trans. Veh. Technol. 60 (2011) 3386–3407.
[6] K.E. Baddour, Y. Bar-Ness, O.A. Dobre, M. Oner, E. Serpedin, U. Spagnolini, Special issue on cognitive radio: The road for its second decade, Phys. Commun. 9 (2013) 145–147.
[7] L. Gavrilovska, D. Denkovski, V. Rakovic, M. Angjelichinoski, Medium access control protocols in cognitive radio networks: Overview and general classification, IEEE Commun. Surv. Tutor. 16 (2014) 2092–2124.
[8] V. Rakovic, V. Atanasovski, L. Gavrilovska, Optimal cooperative spectrum sensing under faded and bandwidth limited control channels, Wirel. Pers. Commun. 78 (2014) 1645–1666.
[9] E. Soltanmohammadi, M. Orooji, M. Naraghi-Pour, Improving the sensing-throughput tradeoff for cognitive radios in rayleigh fading channels, IEEE Trans. Veh. Technol. 62 (2013) 2118–2130.
[10] S. Chaudhari, J. Lunden, V. Koivunen, H. Poor, Cooperative sensing with imperfect reporting channels: Hard decisions or soft decisions? IEEE Trans. Signal Process. 60 (2012) 18–28.
[11] S. Gezici, Z. Sahinoglu, H. Poor, On the optimality of equal gain combining for energy detection of unknown signals, IEEE Commun. Lett. 10 (2006) 772–774.
[12] H. Urkowitz, Energy detection of unknown deterministic signals, Proc. IEEE 55 (1967) 523–531.
[13] F.F. Digham, M.S. Alouini, M.K. Simon, On the energy detection of unknown signals over fading channels, IEEE Trans. Commun. 55 (2007) 21–24.
[14] M. López-Benítez, F. Casadevall, Versatile, accurate, and analytically tractable approximation for the Gaussian Q-function, IEEE Trans. Commun. 59 (2011) 917–922.
[15] A. Makarfi, K. Hamdi, Interference analysis of energy detection for spectrum sensing, IEEE Trans. Veh. Technol. 62 (2013) 2570–2578.
[16] G. Xiong, S. Kishore, A. Yener, Spectrum sensing in cognitive radio networks: Performance evaluation and optimization, Phys. Commun. 9 (2013) 171–183.

[17] P. Sofotasios, E. Rebeiz, L. Zhang, T. Tsiftsis, D. Cabric, S. Freear, Energy detection based spectrum sensing over $\kappa - \mu$ and $\kappa - \mu$ extreme fading channels, IEEE Trans. Veh. Technol. 62 (2013) 1031–1040.
[18] R. Blahut, Hypothesis testing and information theory, IEEE Trans. Inform. Theory 20 (1974) 405–417.
[19] T.M. Cover, J.M. Thomas, Elements of Information Theory, second ed., John Wiley and Sons, Inc., 2005.
[20] J. Tsitsiklis, Decentralized detection by a large number of sensors, Math. Control Signals Systems (MCSS) 1 (1988) 167–182.
[21] J.F. Chamberland, V. Veeravalli, Decentralized detection in sensor networks, IEEE Trans. Signal Process. 51 (2003) 407–416.
[22] Y. Lee, Y. Sung, Generalized Chernoff information for mismatched Bayesian detection and its application to energy detection, IEEE Signal Process. Lett. 19 (2012) 753–756.
[23] P.K. Varshney, Distributed Detection and Data Fusion, first ed., Springer-Verlag New York, Inc., 1996.
[24] I. Maherin, Q. Liang, Radar sensor network for target detection using chernoff information and relative entropy, Phys. Commun. (2014).
[25] Y. Zeng, Y.C. Liang, R. Zhang, Blindly combined energy detection for spectrum sensing in cognitive radio, IEEE Signal Process. Lett. 15 (2008) 649–652.
[26] P. Wang, J. Fang, N. Han, H. Li, Multiantenna-assisted spectrum sensing for cognitive radio, IEEE Trans. Veh. Technol. 59 (2010) 1791–1800.
[27] A. Pandharipande, J. Linnartz, Performance analysis of primary user detection in a multiple antenna cognitive radio, in: Proc. ICC, pp. 6482–6486.
[28] S. Atapattu, C. Tellambura, H. Jiang, Energy detection based cooperative spectrum sensing in cognitive radio networks, IEEE Trans. Wireless Commun. 10 (2011) 1232–1241.
[29] W. Zhang, R. Mallik, K. Letaief, Optimization of cooperative spectrum sensing with energy detection in cognitive radio networks, IEEE Trans. Wireless Commun. 8 (2009) 5761–5766.
[30] G. Sanjeev, K.V.K. Chaythanya, C.R. Murthy, Bayesian decentralized spectrum sensing in cognitive radio networks, in: Int. Conf. on Sig. Proc. and Commun., SPCOM, pp. 1–5.
[31] H. Hashemi, The indoor radio propagation channel, Proc. IEEE 81 (1993) 943–968.
[32] S.J. Shellhammer, N.S. Shankar, R. Tandra, J. Tomcik, Performance of power detector sensors of DTV signals in IEEE 802.22 WRANs, in: Proc. TAPAS, ACM, New York, NY, USA, 2006.
[33] H. Zamat, B. Natarajan, Practical architecture of a broadband sensing receiver for use in cognitive radio, Phys. Commun. 2 (2009) 87–102. Cognitive Radio Networks: Algorithms and System Design.
[34] A. Iyer, K.K. Chintalapudi, V. Navda, R. Ramjee, V. Padmanabhan, C.R. Murthy, Spectrum sensing sans frontières, in: 8th USENIX Symposium on Networked Systems Design and Implementation, NSDI'11.
[35] Y.-C. Liang, Y. Zeng, E. Peh, A.T. Hoang, Sensing-throughput tradeoff for cognitive radio networks, IEEE Trans. Wireless Commun. 7 (2008) 1326–1337.
[36] S. Zheng, P.-Y. Kam, Y.-C. Liang, Y. Zeng, Spectrum sensing for digital primary signals in cognitive radio: A Bayesian approach for maximizing spectrum utilization, IEEE Trans. Wireless Commun. 12 (2013) 1774–1782.
[37] D. Cabric, A. Tkachenko, R. Brodersen, Spectrum sensing measurements of pilot, energy, and collaborative detection, in: Proc. MILCOM, pp. 1–7.
[38] A. Ghasemi, E. Sousa, Collaborative spectrum sensing for opportunistic access in fading environments, in: Proc. DySPAN, pp. 131–136.
[39] S. Mishra, A. Sahai, R. Brodersen, Cooperative sensing among cognitive radios, in: Proc. ICC, vol. 4, pp. 1658–1663.
[40] R. Tandra, A. Sahai, SNR walls for signal detection, IEEE J. Sel. Top. Sign. Proces. 2 (2008) 4–17.
[41] A. Sonnenschein, P.M. Fishman, Radiometric detection of spread-spectrum signals in noise of uncertain power, IEEE Trans. Aerosp. Electron. Syst. 28 (1992) 654–660.
[42] D. Bhargavi, C. Murthy, Performance comparison of energy, matched-filter and cyclostationarity-based spectrum sensing, in: Proc. SPAWC, pp. 1–5.
[43] S. Gurugopinath, C. Murthy, C. Seelamantula, Zero-crossings based spectrum sensing under noise uncertainties, in: Proc. NCC, pp. 1–6.
[44] S. Maleki, S.P. Chepuri, G. Leus, Optimization of hard fusion based spectrum sensing for energy-constrained cognitive radio networks, Phys. Commun. 9 (2013) 193–198.
[45] P. Barsocchi, Channel models for terrestrial wireless communications: A surveym, 2006. Available at: http://puma.isti.cnr.it/dfdownload.php?ident=/cnr.isti/2006-TR-16.
[46] Z. Li, F. Yu, M. Huang, A distributed consensus-based cooperative spectrum-sensing scheme in cognitive radios, IEEE Trans. Veh. Technol. 59 (2010) 383–393.
[47] M. Renzo, L. Imbriglio, F. Graziosi, F. Santucci, Distributed data fusion over correlated log-normal sensing and reporting channels: Application to cognitive radio networks, IEEE Trans. Wireless Commun. 8 (2009) 5813–5821.
[48] Z. Chair, P.K. Varshney, Optimal data fusion in multiple sensor detection systems, IEEE Trans. Aerosp. Electron. Syst. 22 (1986) 98–101.
[49] C. Cordeiro, K. Challapali, D. Birru, S. Shankar, IEEE 802.22: An introduction to the first wireless standard based on cognitive radios, J. Commun. 1 (2006) 38–47.
[50] S. Gurugopinath, C. Murthy, V. Sharma, Error exponent analysis of energy-based Bayesian spectrum sensing under fading channels, in: Proc. Globecom, pp. 1–5.
[51] J. Filho, M. Yacoub, Simple precise approximations to Weibull sums, IEEE Commun. Lett. 10 (2006) 614–616.
[52] M. Di Renzo, F. Graziosi, F. Santucci, Further results on the approximation of log-normal power sum via Pearson type IV distribution: A general formula for log-moments computation, IEEE Trans. Commun. 57 (2009) 893–898.
[53] R. Srinivasan, Importance Sampling: Applications in Communications and Detection, Springer Verlag, 2002.

Sanjeev Gurugopinath received the B.E. degree in Electrical Engineering from Dr. Ambedkar Institute of Technology, Bangalore in 2004, and the M.Tech. degree in Digital Electronics and Communication Engineering from M.S. Ramaiah Institute of Technology, Bangalore in 2006, both from Visvesvaraya Technological University, Belgaum. Since January 2008, he is working towards his Ph.D. at the Signal Processing for Communications Laboratory, at the Electrical Communication Engineering Department, Indian Institute of Science, Bangalore under the supervision of Prof. Chandra R. Murthy.

His research interests are in the areas of detection and estimation theory, information theory and statistics, and cross-layer optimization as applied to spectrum sensing in cognitive radio networks.

Chandra R. Murthy (S'03-M'06-SM'11) received the B.Tech. degree in Electrical Engineering from the Indian Institute of Technology, Madras in 1998, the M.S. and Ph.D. degrees in Electrical and Computer Engineering from Purdue University and the University of California, San Diego, in 2000 and 2006, respectively.

From 2000 to 2002, he worked as an engineer for Qualcomm Inc., where he worked on WCDMA baseband transceiver design and 802.11b baseband receivers. From August 2006 to August 2007, he worked as a staff engineer at Beceem Communications Inc. on advanced receiver architectures for the 802.16e Mobile WiMAX standard. In September 2007, he joined as an assistant professor at the Department of Electrical Communication Engineering at the Indian Institute of Science, where he is currently working.

His research interests are in the areas of Cognitive Radio, Energy Harvesting Wireless Sensors and MIMO systems with channel-state feedback. He is currently serving as an associate editor for the IEEE Signal Processing Letters and as an elected member of the IEEE SPCOM Technical Committee for the years 2014–2016.

Vinod Sharma (SM'00) received his B-Tech in EE in 1978 from Indian Institute of Technology, New Delhi, India and Ph.D. in ECE from Carnegie Mellon University in 1984. He worked in Northeastern University, Boston and University of California in Los Angeles before joining Indian Institute of Science (IISc), Bangalore in 1988 where currently he is a Professor. He has been the chairman of the Electrical communication engineering department at IISc from 2006 to 2011. He is a Fellow of Indian National Academy of Engineers and has received CDAC–ACCS foundation award and the best paper award in National Communication Conference. He is on the editorial boards of three international journals.

His research interests are in Communication Networks, Wireless Communication and Information Theory.